SPANDIDOS PUBLICATIONS

MOLECULAR MEDICINE REPORTS 23: 267, 2021

Procyanidin B2 inhibits lipopolysaccharide-induced apoptosis by suppressing the Bcl-2/Bax and NF-κB signalling pathways in human umbilical vein endothelial cells

DA-QIANG SONG[1*], JIAO LIU[2*], FANG WANG[3*], XIAO-FANG LI[1], MING-HUA LIU[2], ZHUO ZHANG[2], SHOU-SONG CAO[2] and XIAN JIANG[4]

[1]Department of Pharmacy, The Affiliated Hospital of Southwest Medical University; Departments of [2]Pharmacology and [3]Pharmaceutical Analysis, School of Pharmacy, Southwest Medical University; [4]Department of Anesthesiology, The Affiliated Hospital of Southwest Medical University, Luzhou, Sichuan 646000, P.R. China

Received June 25, 2020; Accepted January 4, 2021

DOI: 10.3892/mmr.2021.11906

Abstract. Human umbilical vein endothelial cells (HUVECs) serve a critical role in maintaining normal vascular function. Lipopolysaccharide (LPS), which is released from pathogenic bacteria in the blood, induces HUVEC apoptosis and injury to cause vascular dysfunction and infectious vascular diseases. Procyanidin B2 (PB2) possesses numerous functions, including antioxidant, antitumor, anti-inflammatory and antiapoptosis effects, but the molecular mechanism is not completely understood. The present study investigated the effects of PB2 on LPS-induced cytotoxicity and apoptosis in HUVECs, as well as the underlying mechanisms. The effects of PB2 on LPS-mediated alterations to cytotoxicity, mitochondrial membrane potential, apoptosis were assessed by performing Cell Counting Kit-8, JC-1 fluorescence, Hoechst 33258 staining assays, respectively. IL-1β, IL-6 and TNF-α mRNA expression and protein levels were measured by performing reverse transcription-quantitative PCR and ELISAs, respectively. Bcl-2, Bax, cleaved caspase-3, cleaved caspase-7, cleaved caspase-9, phosphorylated (p)-IκB-α, p-IκB-β, p-NF-κB-p65 and total NF-κB p65 protein expression levels were determined via western blotting. NF-κB p65 nuclear translocation was assessed via immunofluorescence. PB2 pretreatment markedly attenuated LPS-induced cytotoxicity and apoptosis in HUVECs. PB2 also significantly downregulated the expression levels of IL-1β, IL-6, TNF-α, Bax, cleaved caspase-3, cleaved caspase-7, cleaved caspase-9 and p-NF-κB-p65, but upregulated the expression levels of Bcl-2, p-IκB-α and p-IκB-β in LPS-induced HUVECs. Moreover, PB2 markedly inhibited LPS-induced NF-κB p65 nuclear translocation in HUVECs. The results suggested that the potential molecular mechanism underlying PB2 was associated with the Bax/Bcl-2 and NF-κB signalling pathways. Therefore, PB2 may serve as a useful therapeutic for infectious vascular diseases.

Correspondence to: Professor Shou-Song Cao, Department of Pharmacology, School of Pharmacy, Southwest Medical University, 319 Section 3, Zhongshan Road, Luzhou, Sichuan 646000, P.R. China
E-mail: shousongc@gmail.com

Dr Xian Jiang, Department of Anesthesiology, The Affiliated Hospital of Southwest Medical University, 25 Taiping, Luzhou, Sichuan 646000, P.R. China
E-mail: jiangkeke303@163.com

[*]Contributed equally

Abbreviations: PB2, procyanidin B2; HUVECs, human umbilical vein endothelial cells; LPS, lipopolysaccharide; Cyt-c, cytochrome *c*; PDTC, pyrrolidinedithiocarbamate ammonium

Key words: PB2, LPS, apoptosis, NF-κB, cytokine, HUVECs

Introduction

Vascular endothelial cells (VECs), as a selective barrier between tissues and the blood, serve a vital role in maintaining normal vascular function. VEC dysfunction leads to the development of atherosclerosis, arteriolosclerosis, infectious arteritis, Raynaud's disease and thromboangiitis obliterans (1). Lipopolysaccharide (LPS), a bacterial endotoxin, is a common factor that induces VEC injury and dysfunction by triggering an inflammatory reaction and releasing inflammatory factors (2). For example, LPS can significantly decline cell viability and promote cell apoptosis in rat intestine epithelial cells via increasing the levels of cytokines, including TNF-α, IL-6 and IL-10 (3). Moreover, LPS can markedly decreased cell viability and increase apoptosis in murine chondrogenic ATDC5 cells, resulting from the release of several cytokines, including TNF-α, IL-6 and monocyte chemoattractant protein-1 (4). In addition, the secretion of inflammatory cytokines, such as TNF-α and IL-6, can be significantly elevated by LPS in VECs in mice, resulting in induction of cell apoptosis (5).

VEC apoptosis is related to the Bcl-2/Bax and NF-κB signalling pathways (6). The key role of Bcl-2 and caspases is apoptosis regulation (7). Bcl-2 regulates cellular apoptosis by controlling the permeability of cellular mitochondria. Bcl-2 serves as an antiapoptotic protein in the outer mitochondrial

wall to inhibit cytochrome *c* (Cyt-c) release. By contrast, Bax, a proapoptotic protein, transfers from the cytosol to the mitochondria to promote Cyt-c release from mitochondria, resulting in apoptosis induction and DNA damage (8). Previous studies have demonstrated that apoptosis induction by stimuli is associated with the Bcl-2/Bax signalling pathway, and perfluorocarbon decreased blast injury-induced cell damage by inhibiting the Bcl-2/Bax, NF-κB and MAPK signalling pathways in A549 cells (9-13). The caspase family are apoptosis-specific targets, and as cysteine-aspartic acid proteases, caspase-3 and caspase-7 directly induce apoptosis after sequential activation (14).

As a protein complex, NF-κB controls DNA transcription, cytokine production, cell survival and apoptosis, and dysregulation of NF-κB signalling can lead to inflammation, autoimmune disease and cancer (15). NF-κB is translocated into the nucleus to activate multiple target genes involved in proliferation and apoptosis (16). In the early stages of apoptosis, NF-κB protects against heat stress-induced apoptosis in HUVECs (17). IκB-α and IκB-β are major signal-responsive isoforms in the IκB family (18). IκB-α is a critical regulator of NF-κB and one of the first genes induced following NF-κB activation (19). When activated, IκB-α enters the nucleus to remove NF-κB from gene promoters and transport NF-κB proteins back to the cytoplasm for feedback regulation (20). IκB-β activates NF-κB transcription factors by phosphorylation of IκB inhibitors (21).

Procyanidin B2 (epicatechin-(4β-8)-epicatechin; PB2), a phenolic compound, primarily exists in common fruits, including red grapes, cocoa, lindera aggregate and cinnamon (22). PB2 isolated from cinnamon can significantly decline cell viability and accelerate apoptosis in prostate cancer cells, and the proapoptotic effect of PB2 might be associated with caspase-3 activity (23). PB2 is a bioactive component and a potent antioxidant for restoring and maintaining homeostasis (24). PB2 displays anti-inflammatory and antiapoptotic effects via the regulation of various cytokines and other inflammatory mediators (25). PB2 extracted from fruits and red wine displays potential anti-inflammatory activities. For example, PB2 dramatically inhibits NLR family pyrin domain containing 3 (NLRP3) inflammasome activation and further reduces subsequent activation of caspase-1 or secretion of the inflammatory cytokine IL-1β, resulting from inhibition of the activator protein-1 signalling pathway in HUVECs (26). PB2 can suppress LPS-induced inflammation and apoptosis in human type II alveolar epithelial cells, which is related to inhibition of inflammatory cytokines, including TNF-α and IL-1β, as well as activation of NF-κB and the NLRP3 inflammasome (27). However, the effects of PB2 on the NF-κB or Bcl-2/Bax signalling pathways, and the expression of related cytokines are not completely understood. The results of the aforementioned studies suggest that PB2 displays protective effects in HUVECs (26). Procyanidin protects against glycated low-density lipoprotein-induced apoptosis and LPS-induced acute gut injury via regulating the oxidative state (28,29). However, the mechanism underlying the anti-inflammatory and antiapoptotic effects of PB2 is not completely understood. Therefore, the present study investigated the protective effects of PB2 on LPS-induced cytotoxicity and apoptosis in HUVECs, as well as the underlying mechanisms.

Materials and methods

Cell culture. HUVECs (Procell Life Science & Technology Co. Ltd.) were cultured in DMEM supplemented with 10% FBS and 1% streptomycin/penicillin (all purchased from Thermo Fisher Scientific, Inc.) in a humidified incubator with 95% air and 5% CO_2 at 37˚C. Cell culture medium was replaced every 2-3 days.

Drug preparation. PB2 (Push Bio-Technology) was dissolved in endotoxin-free ultrapure water to make a 20 μg/ml stock solution. LPS (Sigma-Aldrich; Merck KGaA) was dissolved in endotoxin-free ultrapure water to make a 1 mg/ml stock solution. Pyrrolidine dithiocarbamate (PDTC), a specific NF-κB inhibitor, was used as a positive control for PB2. PDTC (Sigma-Aldrich; Merck KGaA) was also dissolved in endotoxin-free ultrapure water to make a 4 μg/ml stock solution. All stock solutions were stored at -20˚C until use.

Cell treatment. HUVECs cultured as described above for 24 h were divided into six groups: i) Vehicle control group, cells were treated with free-serum medium for 24 h; ii) LPS group, cells were incubated in serum-free medium for 12 h, followed by treatment with 1 μg/ml LPS for 12 h; iii) PB2 group, cells were incubated in serum-free medium for 12 h followed by treatment with 5 μg/ml PB2 for 12 h; iv) PDTC group, cells were incubated in serum-free medium for 12 h followed by treatment with 2 μg/ml PDTC for 12 h; v) LPS + PB2 group, cells were treated with 5 μg/ml PB2 for 12 h, followed by 1 μg/ml LPS for 12 h; and vi) LPS + PDTC group, cells were treated with 2 μg/ml PDTC for 12 h, followed by 1 μg/ml LPS for 12 h. All treatments were performed at a constant temperature of 35˚C.

Assessment of cell viability via the cell counting Kit-8 (CCK-8) assay. The effects of LPS, PDTC and PB2 on HUVEC viability were detected by performing the CCK-8 assay, as previously described (30,31). Briefly, HUVECs were seeded ($5x10^4$ cells/well) into 96-well plates and cultured in DMEM containing 10% FBS for 24 h. Subsequently, cells were cultured in serum-free DMEM medium for 12 h, and then treated with serum-free medium (vehicle control), PDTC (2 μg/ml), PB2 (1.25-10 μg/ml) (32) or LPS (1 μg/ml) for 12 h. For combination treatment, cells were treated with PDTC (2 μg/ml) or PB2 (5 μg/ml) for 12 h, followed by treatment with LPS (1 μg/ml) for 12 h. Subsequently, 10 μl CCK-8 solution (Beijing Solarbio Science & Technology Co., Ltd.) was added to each well and incubated for 1 h. The absorbance was measured at a wavelength of 450 nm using a SpectraMax M3 microplate reader (Molecular Devices, LLC).

Analysis of HUVEC apoptosis via Hoechst 33258 staining. Apoptotic cells were detected using a Hoechst 33258 staining kit (Beyotime Institute of Biotechnology) according the manufacturer's protocol. Briefly, HUVECs were seeded ($1x10^5$ cells/well) into 6-well plates and cultured in DMEM for 12 h. Cells were then treated with serum-free medium (control), LPS (1 μg/ml), PDTC (2 μg/ml) or PB2 (1.25-10 μg/ml) for 12 h. For combination treatment, cells were treated with PDTC (2 μg/ml) or PB2 (5 μg/ml) for 12 h, followed by treatment with LPS (1 μg/ml) for 12 h. Subsequently, cells were incubated

with 4% paraformaldehyde for 10 min at room temperature (25˚C), washed with PBS for 15 min and treated with 10 μg/ml Hoechst 33258 staining solution (500 μl/well) for 5 min at room temperature (25˚C). Following washing with PBS for 15 min in the dark, the nuclear morphology of apoptotic cells was observed using an AMG EVOS fluorescent microscope (Thermo Fisher Scientific Inc.; magnification, x400). The percentage (%) of apoptotic cells was calculated as the ratio of apoptotic cells to total cells.

Analysis of IL-1β, IL-6 and TNF-α mRNA expression levels via reverse transcription-quantitative PCR (RT-qPCR) in HUVECs. HUVECs were seeded (1x10^5 cells/well) into flasks and cultured in DMEM for 24 h, followed by culture in serum-free DMEM for 12 h. Subsequently, cells were treated with serum-free medium (vehicle control), LPS (1 μg/ml), PB2 (5 μg/ml) or PDTC (2 μg/ml) for 12 h. For combination treatment, cells were treated with PB2 (5 μg/ml) or PDTC (2 μg/ml) for 12 h, washed with PBS for 15 min at room temperature and treated with LPS (1 μg/ml) for 12 h. Total RNA was extracted from cells using the RNAsimple Total RNA kit (Tiangen Biotech Co., Ltd.) according to the manufacturer's protocol. Total RNA (1 μg) was reverse transcribed into cDNA using the TIANScript RT kit (Tiangen Biotech Co., Ltd.), according to the manufacturer's protocol. Subsequently, qPCR was performed using 1 μl cDNA in a 20-μl total reaction volume using SuperReal PreMix Plus (SYBR Green Real Time PCR Mix; Tiangen Biotech Co., Ltd.) and the 7900HT Fast Real-Time PCR system (Applied Biosystems; Thermo Fisher Scientific, Inc.). The following thermocycling conditions were used for qPCR: 95˚C for 10 min; 45 cycles (95˚C for 15 sec and 60˚C for 1 min per cycle). The primers used for qPCR were designed using Primer Premier (version 5.0; Premier Biosoft International): IL-1β forward, 5'-ATGATGGCTTATTACAGTGGCAA-3' and reverse, 5'-GTCGGAGATTCGTAGCTGGA-3' (amplicon size, 132 bp); IL-6 forward, 5'-ACTCACCTCTTCAGAACGAATTG-3' and reverse, 5'-CCATCTTTGGAAGGTTCAGGTTG-3' (amplicon size, 149 bp); TNF-α forward, 5'-AGGACCAGCTAAGAG GGAGA-3' and reverse, 5'-CCCGGATCATGCTTTCAGTG-3' (amplicon size, 136 bp); and GAPDH forward, 5'-CTCACC GGATGCACCAATGTT-3' and reverse, 5'-CGCGTTGCTCAC AATGTTCAT-3' (amplicon size, 82 bp) (Sangon Biotech Co., Ltd.). mRNA expression levels were normalized to the internal reference gene GAPDH. The results were calculated using CFX Manager software (version 3.1; Bio-Rad Laboratories, Inc.) and quantified using the $2^{-\Delta\Delta Cq}$ method (33).

Analysis of IL-1β, IL-6 and TNF-a protein levels via ELISA in HUVECs. IL-1β, IL-6 and TNF-α protein levels in HUVECs were measured using ELISA kits according to manufacturers' protocols. Briefly, HUVECs were seeded (1x10^5 cells/well) into 6-well plates and cultured in DMEM for 12 h, followed by culture in serum-free DMEM for 12 h. Subsequently, cells were treated with serum-free medium (vehicle control), LPS (1 μg/ml), PB2 (5 μg/ml) or PDTC (2 μg/ml) for 12 h. For combination treatment, cells were treated with PB2 (5 μg/ml) or PDTC (2 μg/ml) for 12 h prior to treatment with LPS (1 μg/ml) for 12 h. To harvest the cytokines secreted by cells in each group, the cell suspensions were centrifuged at 3,000 x g at room temperature (25˚C) for 5 min. The protein levels of IL-1β, IL-6, and TNF-a in the supernatants were detected using the following ELISA kits (R&D Systems, Inc.): Human IL-1β QuantiGlo ELISA kit (cat. no. QLB00B), human IL-6 Quantikine ELISA kit (cat. no. PD6050) and human TNF-α Quantikine ELISA kit (cat. no. PDTA00D). The absorbance was measured at a wavelength of 450 nm using a SpectraMax M3 microplate reader (Molecular Devices, LLC).

Western blotting. HUVECs were seeded (1x10^5 cells/well) into flasks and cultured in DMEM for 24 h, followed by culture in serum-free DMEM for 12 h. Cells were treated with serum-free medium (control), LPS (1 μg/ml), PB2 (5 μg/ml) or PDTC (2 μg/ml) for 12 h. For combination treatment, cells were treated with PB2 (5 μg/ml) or PDTC (2 μg/ml) for 12 h, washed with PBS for 15 min at room temperature and then treated with LPS (1 μg/ml) for 12 h. The culture medium was removed, and cells were washed with cold PBS. Total protein was extracted from cells using RIPA lysis buffer (0.5% NP-40, 50 mM Tris-HCl, 120 mM NaCl, 1 mM EDTA, 0.1 mM Na3VO4, 1 mM NaF, 1 mM PMSF; and 1 μg/ml leupeptin; pH 7.5). Cell lysates were centrifuged at 10,000 x g for 20 min at 4˚C. Protein quantification was performed using a BCA assay, then proteins (~30 μg) were separated via 12% SDS-PAGE and electrotransferred to PVDF membranes. Following blocking with 5% skimmed milk in TBS-0.1% Tween 20 for 1 h at room temperature (25˚C), the membranes were incubated overnight at 4˚C with primary antibodies (all 1:1,000; Cell Signaling Technology, Inc.) diluted in primary antibody dilution buffer (Beyotime Institute of Biotechnology) targeted against Bcl-2 (cat. no. 4223), Bax (cat. no. 2774), cleaved caspase-3 (cat. no. 9661), cleaved caspase-7 (cat. no. 8438), cleaved caspase-9 (cat. no. 20750), phosphorylated (p)-IκB-α (cat. no. 2859), total IκB-α (cat. no. 9242), p-IκB-β (cat. no. 4921), total IκB-β (cat. no. 15519), p-NF-κB p65 (cat. no. 3033), total NF-κB p65 (cat. no. 8242) and β-actin (cat. no. 4970S). Following washing three times with TBST, the membranes were incubated at room temperature with an anti-rabbit IgG, HRP-conjugated antibody (1:5,000; cat. no. 7074; Cell Signaling Technology, Inc.) for 1 h with gentle agitation at room temperature. The membranes were washed three times with TBST for 30 min. Subsequently, protein bands were visualized using ECL western detection reagents (Thermo Fisher Scientific, Inc.). Protein expression levels were semi-quantified using ImageJ v1.8.0 software (National Institutes of Health).

Analysis of nuclear translocation of NF-κB p65 via immunofluorescence in HUVECs. HUVECs were seeded (1x10^5 cells/well) into 6-well plates, cultured in DMEM for 24 h, followed by culture in serum-free DMEM for 12 h. Cells were then treated with serum-free medium (control), LPS (1 μg/ml), PB2 (5 μg/ml) or PDTC (2 μg/ml). For combination treatment, cells were treated with PB2 (5 μg/ml) or PDTC (2 μg/ml) for 12 h, washed with PBS for 15 min at room temperature and then treated with LPS (1 μg/ml) for 12 h. Cells were washed with PBS for 10 min at room temperature and fixed in 4% paraformaldehyde at 4˚C for 30 min. Following washing three times with PBS for 5 min each time, cells were incubated with 0.1% Triton X-100 for 10 min at room temperature (25˚C) and blocked with 1% BSA (Beyotime Institute of Biotechnology) for 30 min at room temperature (25˚C). Cells were incubated with an anti-NF-κB

p65 rabbit monoclonal primary antibody (cat. no. 8801; 1:500; Cell Signaling Technology, Inc.) at 4˚C overnight. Subsequently, cells were incubated with an HRP-conjugated goat anti-rabbit secondary antibody (1:2,000; Cell Signaling Technology, Inc.) for 2 h at room temperature (25˚C). Following washing with PBS for 15 min, cells were stained with DAPI for 10 min at room temperature (25˚C) and washed with PBS for 15 min. Stained cells were visualized using a CKX41 inverted phase contrast fluorescence microscope (Olympus Corporation; magnification, x400).

Statistical analysis. Statistical analyses were performed using SPSS software (version 20.0; IBM Corp.). Data are presented as the mean ± SD. All experiments were repeated three times in triplicate. Comparisons among multiple groups were analysed using one-way ANOVA followed by Tukey's post hoc test. P<0.05 was considered to indicate a statistically significant difference.

Results

Protective effect of PB2 on LPS-induced inhibition of HUVEC viability. The effects of PB2, PDTC and LPS on HUVEC viability were evaluated by performing the CCK-8 assay (Fig. 1B and C). Compared with the vehicle control group, PB2 (≤5 μg/ml) and PDTC (2 μg/ml) displayed no significant inhibitory effect on cell viability, resulting in >95% cell viability. However, PB2 (10 μg/ml) significantly inhibited cell viability, resulting in 69.67±6.28% cell viability compared with the vehicle control (98.46±3.23% cell viability).

Subsequently, the protective effects of PB2 and PDTC on LPS-induced cytotoxicity were assessed. The results demonstrated that pretreatment with PB2 or PDTC notably protected cells against LPS-induced cytotoxicity in HUVECs (Fig. 1C). The results indicated that PB2 and PDTC effectively protected against LPS-induced inhibition of HUVEC viability.

Effect of PB2 on LPS-induced HUVEC apoptosis. Hoechst 33258 staining is used for the rapid detection of cellular apoptosis by observing chromatin condensation via fluorescence microscopy (34). Therefore, the protective effect of PB2 on LPS-induced apoptosis was assessed by performing Hoechst 33258 staining assays.

The vehicle control group displayed typical features of HUVECs as demonstrated by normal blue fluorescence in the cell nuclei (Fig. 2A). However, apoptotic cells with condensation of nuclear chromatin and fragmentation, which were stained white, were observed in LPS-treated cells. The percentage of apoptotic cells was clearly reduced in LPS-treated cells pretreated with PB2 or PDTC compared with cells treated with LPS alone (Fig. 2B). However, PB2 or PDTC treatment alone displayed no significant effect on HUVEC apoptosis compared with vehicle control group. LPS significantly induced apoptosis (70.67±2.12% apoptotic cells) compared with the vehicle control group (6.41±1.26% apoptotic cells); however, PB2 or PDTC pretreatment notably attenuated LPS-induced HUVEC apoptosis. The results indicated that PB2 markedly inhibited LPS-induced HUVEC apoptosis.

PB2 reverses LPS-induced reductions in the mitochondrial membrane potential in HUVECs. A previous study

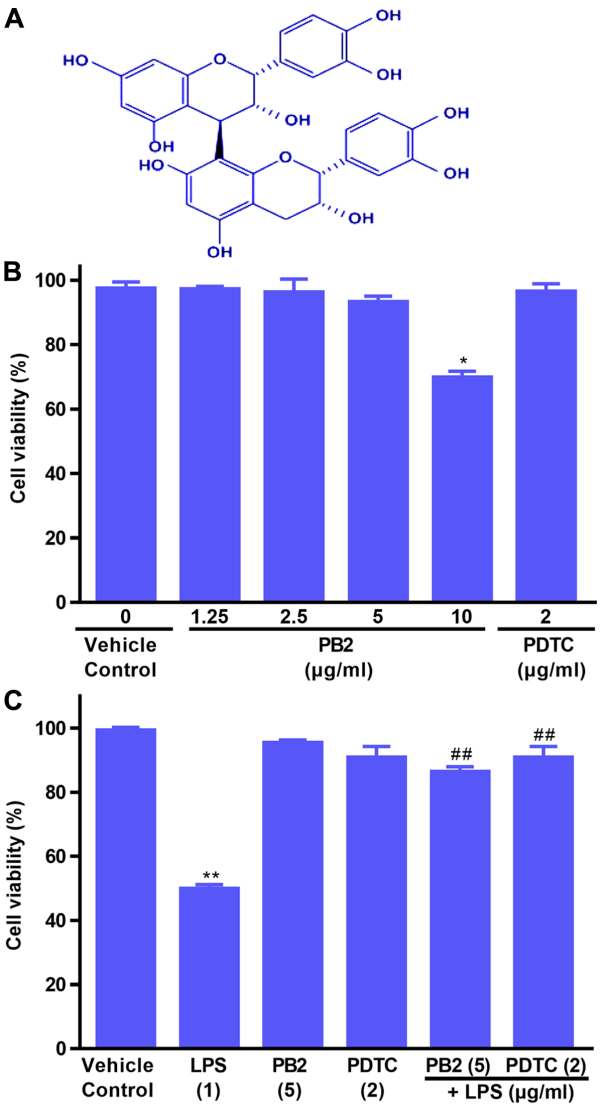

Figure 1. Chemical structure of PB2, and the effects of LPS, PB2 and PDTC on HUVEC viability. Cells were treated with serum-free medium for 24 h (vehicle control) or with serum-free medium for 12 h followed by LPS (1 μg/ml) for 12 h, PB2 (1.25-10 μg/ml) or PDTC (2 μg/ml) for 12 h followed by serum-free medium or LPS for 12 h. (A) Chemical structure of PB2. (B) Effects of PB2 and PDTC on HUVEC viability. (C) Effects of LPS, PB2 and PDTC on HUVEC viability. Data are presented as the mean ± SD of at least three independent experiments run in triplicate (n=3). Data were analysed using one-way ANOVA followed by Tukey's post hoc test. *P<0.05, **P<0.01 vs. vehicle control; $^{\#\#}$P<0.01 vs. LPS. PB2, procyanidin B2; LPS, lipopolysaccharide; PDTC, pyrrolidinedithiocarbamate ammonium; HUVEC, human umbilical vein endothelial cell.

demonstrated that declined mitochondrial membrane potential is a hallmark of early apoptosis (35). Therefore, the effects of PB2 on LPS-induced reductions in the mitochondrial membrane potential in HUVECs were assessed via JC-1 fluorescence. The red fluorescence intensity and red/green ratio were significantly reduced by LPS compared with the vehicle control group in HUVECs (Fig. 3). The red fluorescence intensity and ratio of red/green fluorescence were notably increased in cells treated with PB2 or PDTC compared with the LPS group. The results demonstrated that compared with the vehicle control group, LPS significantly decreased the mitochondrial membrane potential, but pretreatment with PB2 or PDTC reversed LPS-mediated effects on the mitochondrial

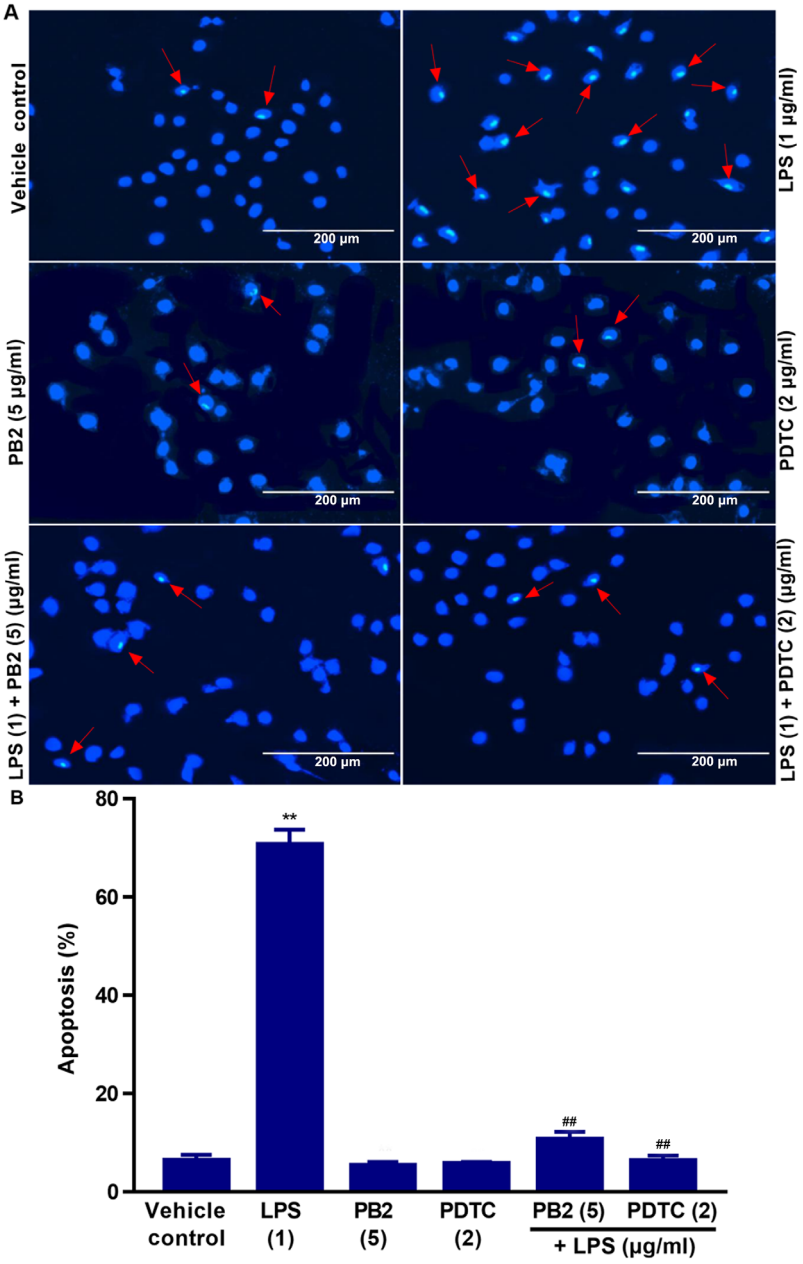

Figure 2. Effects of PB2 and PDTC on LPS-induced HUVEC apoptosis. Cells were treated with serum-free medium alone for 24 h in the vehicle control group; cells were treated with serum-free medium for 12 h followed by LPS (1 μg/ml) for 12 h in the LPS group; cells were treated with serum-free medium for 12 h followed by PB2 (5 μg/ml) for 12 h in the PB2 group; cells were treated with serum-free medium for 12 h followed by PDTC (2 μg/ml) for 12 h in the PDTC group; cells were treated with PB2 (5 μg/ml) for 12 h followed by LPS (1 μg/ml) for 12 h in the LPS + PB2 group; cells were treated with PDTC (2 μg/ml) for 12 h followed by LPS (1 μg/ml) for 12 h in the LPS + PDTC group. (A) Representative images of apoptotic cells identified by Hoechst staining via fluorescence microscopy (magnification, x400). Red arrows indicate apoptotic cells. The vehicle control group displayed the typical features of HUVECs with the appearance of normal blue fluorescence in the cell nuclei. In LPS-treated HUVECs, apoptotic cells with condensation of nuclear chromatin and fragmentation, which was indicated by white staining, were observed. Pretreatment with PB2 or PDTC prior to LPS treatment markedly reduced the number of apoptotic cells compared with the LPS group. However, PB2 or PDTC treatment alone displayed no obvious effect on HUVEC apoptosis compared with the vehicle control group. (B) Quantification of the percentage of apoptotic cells. Data are presented as the mean ± SD of at least three independent experiments run in triplicate (n=3). Data were analysed using one-way ANOVA followed by Tukey's post hoc test. **P<0.01 vs. vehicle control; $^{\#\#}$P<0.01 vs. LPS. PB2, procyanidin B2; PDTC, pyrrolidinedithiocarbamate ammonium; LPS, lipopolysaccharide; HUVEC, human umbilical vein endothelial cell.

membrane potential in HUVECs. Therefore, the results suggested that PB2-induced inhibition of LPS-induced apoptosis might be mediated, at least in part, via attenuating LPS-induced reductions in the mitochondrial membrane potential in HUVECs.

Effect of PB2 on LPS-induced upregulation of IL-1β, IL-6 and TNF-α mRNA expression levels in HUVECs. Key proinflammatory cytokines, including IL-1β, IL-6 and TNF-α, are involved in a variety of cellular activities, such as proliferation, differentiation and apoptosis, and serve an important role in the immune response to inflammation (36). LPS can stimulate the production of IL-1β, IL-6, and TNF-α via different modes in human monocytes/macrophages (37). Therefore, the effect of PB2 on LPS-induced upregulation of IL-1β, IL-6 and TNF-α mRNA expression levels was assessed.

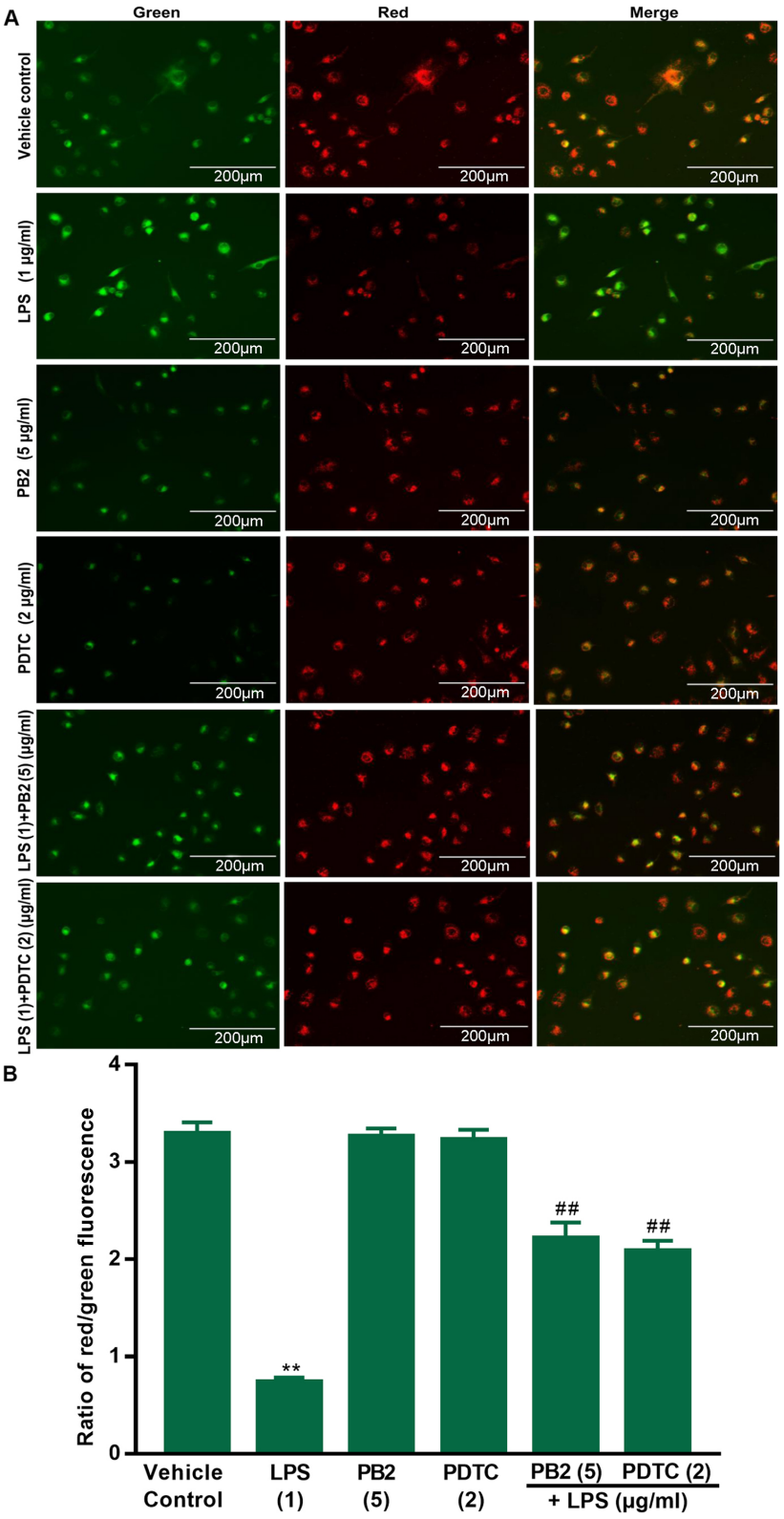

Figure 3. Effects of LPS, PB2 and PDTC on mitochondrial membrane potential in HUVECs. Cells were treated with serum-free medium for 24 h in the vehicle control group; cells were treated with serum-free medium for 12 h followed by LPS (1 μg/ml) for 12 h in the LPS group; cells were treated with serum-free medium for 12 h followed by PB2 (5 μg/ml) for 12 h in the PB2 group; cells were treated with serum-free medium for 12 h followed by PDTC (2 μg/ml) for 12 h in the PDTC group; cells were treated with PB2 (5 μg/ml) for 12 h followed by LPS (1 μg/ml) for 12 h in the LPS + PB2 group; cells were treated with PDTC (2 μg/ml) for 12 h followed by LPS (1 μg/ml) for 12 h in the LPS + PDTC group. (A) Representative images of mitochondrial membrane potential identified using JC-1 fluorescent dye (green as a monomer; red-orange as a dimer) via fluorescence microscopy (magnification, x400). (B) Quantification of the ratio of red/green fluorescence. The red fluorescence intensity and ratio of red/green fluorescence were notably increased in LPS-treated cells pretreated with PB2 or PDTC compared with cells treated with LPS alone. Compared with the vehicle control group, LPS significantly decreased the mitochondrial membrane potential, but pretreatment with PB2 and PDTC reversed LPS-induced reductions in the mitochondrial membrane potential in HUVECs. Data are presented as the mean ± SD of at least three independent experiments run in triplicate (n=3). Data were analysed using one-way ANOVA followed by Tukey's post hoc test. **P<0.01 vs. vehicle control; $^{\#\#}$P<0.01 vs. LPS. LPS, lipopolysaccharide; PB2, procyanidin B2; PDTC, pyrrolidinedithiocarbamate ammonium; HUVEC, human umbilical vein endothelial cell.

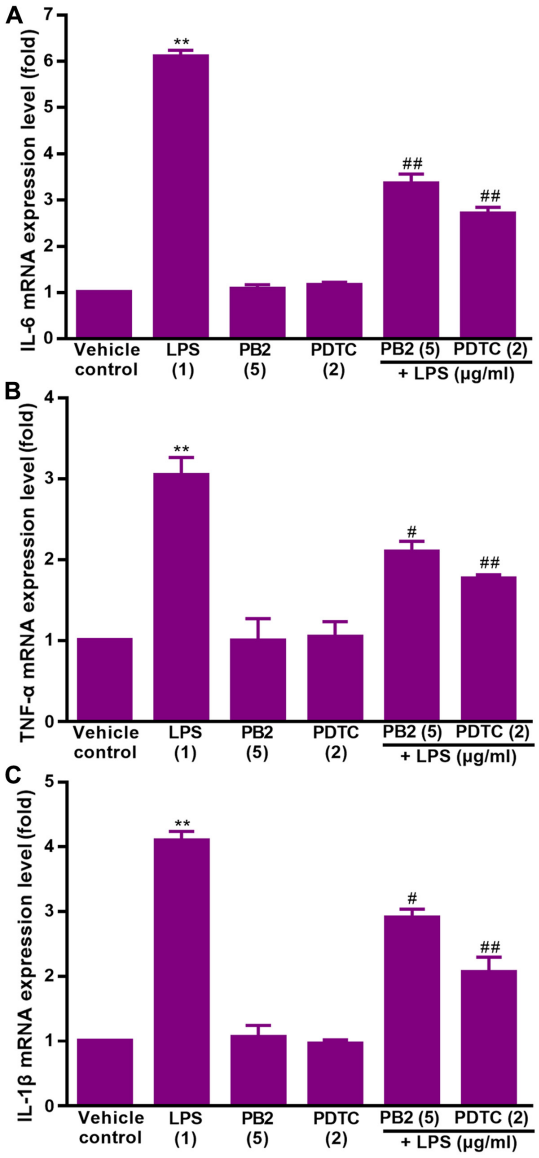

Figure 4. Effect of LPS, PB2 and PDTC on the mRNA expression levels of inflammatory cytokines in HUVECs. Cells were treated with serum-free medium for 24 h in the vehicle control group; cells were treated with serum-free medium for 12 h followed by LPS (1 μg/ml) for 12 h in the LPS group; cells were treated with serum-free medium for 12 h followed by PB2 (5 μg/ml) for 12 h in the PB2 group; cells were treated with serum-free medium for 12 h followed by PDTC (2 μg/ml) for 12 h in the PDTC group; cells were treated with PB2 (5 μg/ml) for 12 h followed by LPS (1 μg/ml) for 12 h in the LPS + PB2 group; cells were treated with PDTC (2 μg/ml) for 12 h followed by LPS (1 μg/ml) for 12 h in the LPS + PDTC group. (A) IL-6, (B) TNF-α and (C) IL-1β mRNA expression levels were measured via reverse transcription-quantitative PCR in HUVECs. mRNA expression levels were normalized to the internal reference gene GAPDH. Data are presented as the mean ± SD of at least three independent experiments run in triplicate (n=3). Data were analysed using one-way ANOVA followed by Tukey's post hoc test. **P<0.01 vs. vehicle control; $^{\#}$P<0.05, $^{\#\#}$P<0.01 vs. LPS. LPS, lipopolysaccharide; PB2, procyanidin B2; PDTC, pyrrolidinedithiocarbamate ammonium; HUVEC, human umbilical vein endothelial cell.

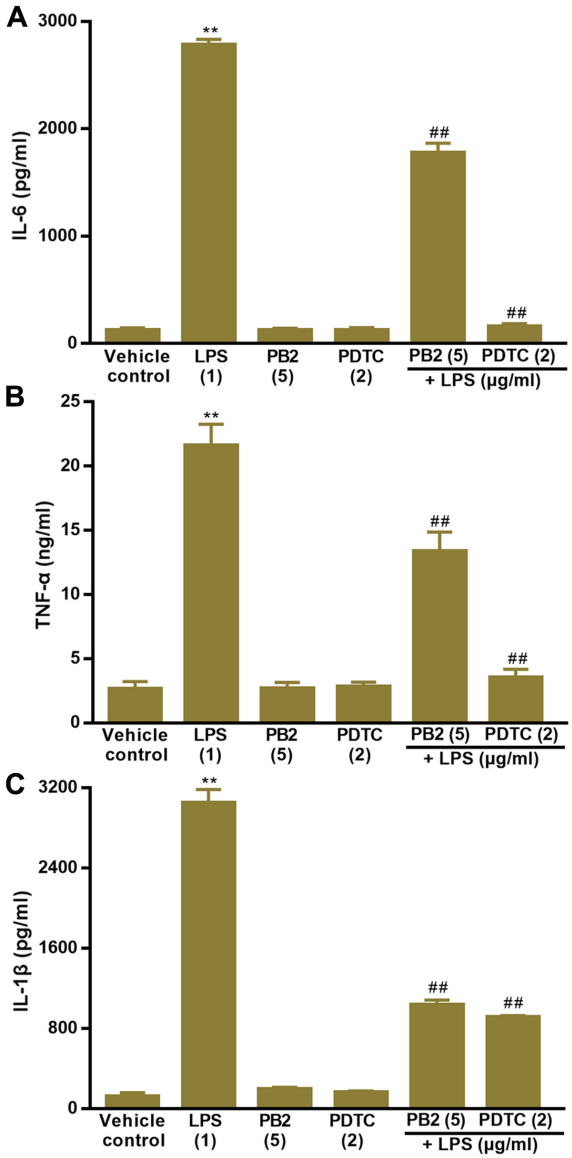

Figure 5. Effect of LPS, PB2 and PDTC on the protein expression levels of inflammatory cytokines in HUVECs. Cells were treated with serum-free medium for 24 h in the vehicle control group; cells were treated with serum-free medium for 12 h followed by LPS (1 μg/ml) for 12 h in the LPS group; cells were treated with serum-free medium for 12 h followed by PB2 (5 μg/ml) for 12 h in the PB2 group; cells were treated with serum-free medium for 12 h followed by PDTC (2 μg/ml) for 12 h in the PDTC group; cells were treated with PB2 (5 μg/ml) for 12 h followed by LPS (1 μg/ml) for 12 h in the LPS + PB2 group; cells were treated with PDTC (2 μg/ml) for 12 h followed by LPS (1 μg/ml) for 12 h in the LPS + PDTC group. (A) IL-6, (B) TNF-α and (C) IL-1β protein expression levels in HUVECs were detected by performing ELISAs. Data are presented as the mean ± SD of at least three independent experiments run in triplicate (n=3). Data were analysed using one-way ANOVA followed by Tukey's post hoc test. **P<0.01 vs. vehicle control; $^{\#\#}$P<0.01 vs. LPS. LPS, lipopolysaccharide; PB2, procyanidin B2; PDTC, pyrrolidinedithiocarbamate ammonium; HUVEC, human umbilical vein endothelial cell.

The effect of PB2 on LPS-induced upregulation of IL-1β, IL-6 and TNF-α mRNA expression levels in HUVECs was assessed via RT-qPCR (Fig. 4). The results demonstrated that IL-1β, IL-6 and TNF-α mRNA expression levels were significantly increased by LPS compared with the vehicle control group, but pretreatment of LPS-treated cells with PB2 or PDTC notably reversed LPS-induced alterations to mRNA expression levels in HUVECs.

Effect of PB2 on LPS-induced upregulation of IL-1β, IL-6 and TNF-α protein levels in HUVECs. The effect of PB2 on LPS-induced increases in IL-1β, IL-6 and TNF-α protein levels was assessed by performing ELISAs (Fig. 5). The results also

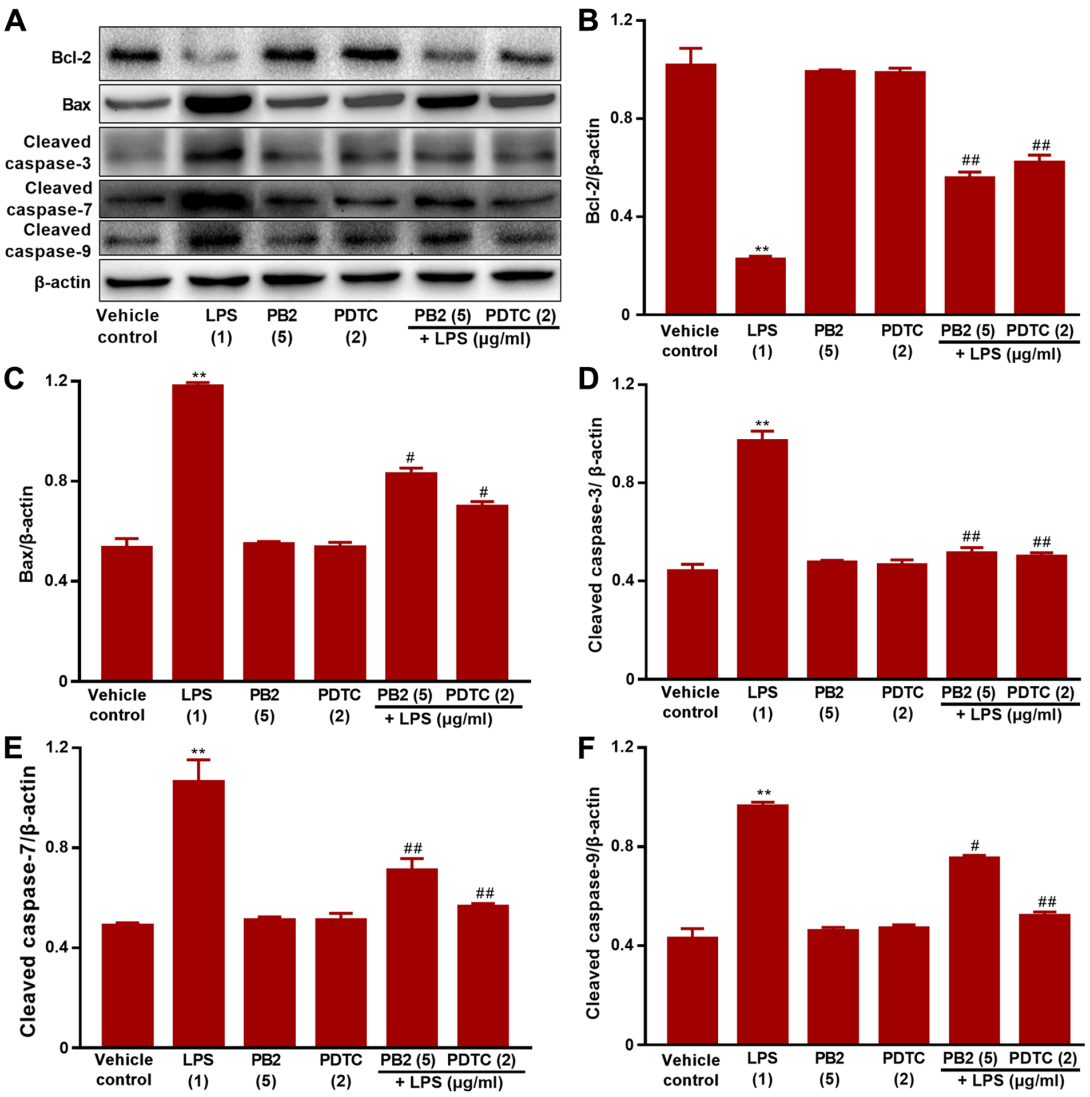

Figure 6. Effects of LPS, PB2 and PDTC on Bcl-2, Bax, cleaved caspase-3, cleaved caspase-7 and cleaved caspase-9 protein expression levels in HUVECs. Cells were treated with serum-free medium for 24 h in the vehicle control group; cells were treated with serum-free medium for 12 h followed by LPS (1 μg/ml) for 12 h in the LPS group; cells were treated with serum-free medium for 12 h followed by PB2 (5 μg/ml) for 12 h in the PB2 group; cells were treated with serum-free medium for 12 h followed by PDTC (2 μg/ml) for 12 h in the PDTC group; cells were treated with PB2 (5 μg/ml) for 12 h followed by LPS (1 μg/ml) for 12 h in the LPS + PB2 group; cells were treated with PDTC (2 μg/ml) for 12 h followed by LPS (1 μg/ml) for 12 h in the LPS + PDTC group. Protein expression levels in HUVECs were (A) determined via western blotting and semi-quantified for (B) Bcl-2, (C) Bax, (D) cleaved caspase-3, (E) cleaved caspase-7 and (F) cleaved caspase-9. β-actin was used as the loading control. Data are presented as the mean ± SD of at least three independent experiments run in triplicate (n=3). Data were analysed using one-way ANOVA followed by Tukey's post hoc test. **P<0.01 vs. vehicle control; $^{\#}$P<0.05, $^{\#\#}$P<0.01 vs. LPS. LPS, lipopolysaccharide; PB2, procyanidin B2; PDTC, pyrrolidinedithiocarbamate ammonium; HUVEC, human umbilical vein endothelial cell.

demonstrated that IL-1β, IL-6 and TNF-α protein levels were significantly increased by LPS compared with the vehicle control group in HUVECs. However, pretreatment of LPS-treated cells with PB2 or PDTC clearly decreased LPS-induced increases in the protein levels of IL-1β, IL-6 and TNF-α in HUVECs.

Effect of PB2 on the Bcl-2/Bax signalling pathway in HUVECs. The Bcl-2/Bax signalling pathway serves a critical role in apoptosis (38). It was hypothesized that the antiapoptotic effect of PB2 might be mediated via regulating the Bcl-2/Bax signalling pathway. Therefore, the effects of PB2 on Bcl-2, Bax, cleaved caspase-3, cleaved caspase-7 and cleaved caspase-9 expression levels in HUVECs were analysed via western blotting (Fig. 6). The protein expression levels of Bax, cleaved caspase-3, cleaved caspase-7 and cleaved caspase-9 were significantly upregulated, but Bcl-2 protein expression levels were significantly downregulated by LPS compared with the vehicle control, PDTC or PB2 groups. Moreover, pretreatment with PB2 notably reversed LPS-induced elevations in the protein expression levels of Bax, cleaved caspase-3, cleaved caspase-7 and cleaved caspase-9, but upregulated the protein expression levels of Bcl-2. The results obtained from the pretreatment with PDTC was similar to that of PB2. The results suggested that the antiapoptotic effect of PB2 was related to the Bcl-2/Bax signalling pathway in HUVECs.

Effect of PB2 on inhibition of the NF-κB signalling pathway in HUVECs. The NF-κB signalling pathway serves a vital role in regulating cell survival, apoptosis and cytokine production (17).

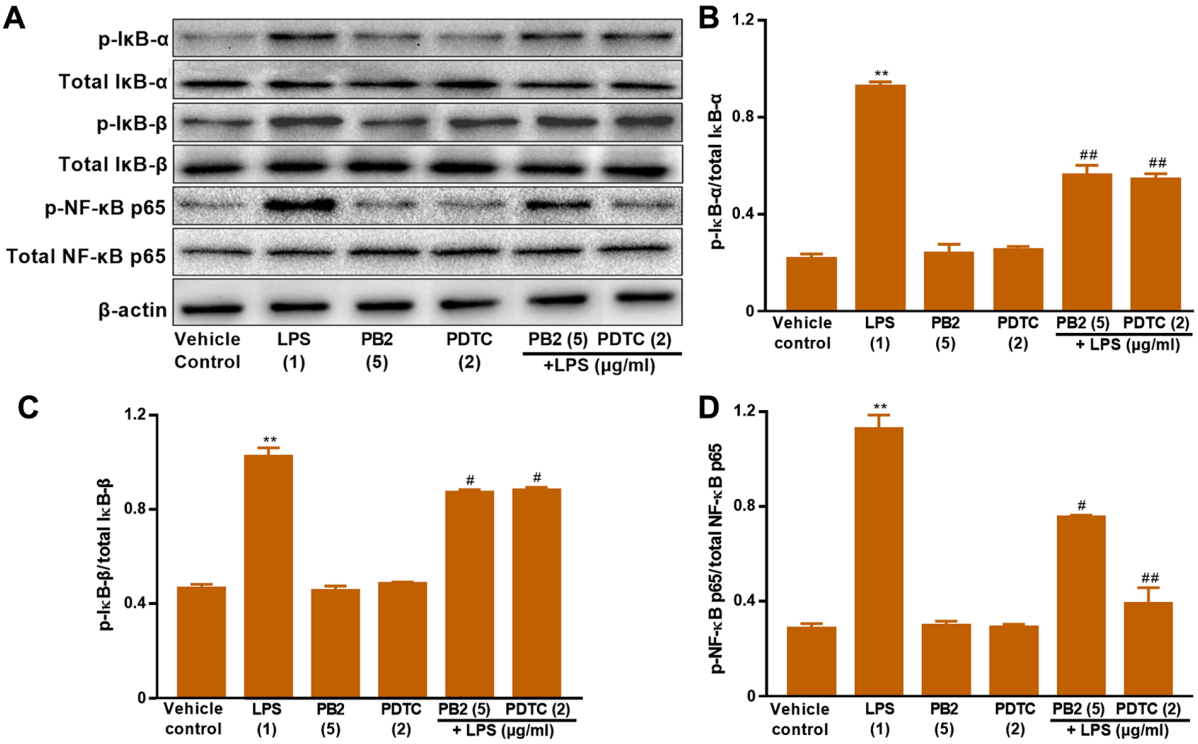

Figure 7. Effects of LPS, PB2 and PDTC on p-IκB-α, p-IκB-β, p-NF-κB p65 and total NF-κB p65 protein expression levels in HUVECs. Cells were treated with serum-free medium for 24 h in the vehicle control group; cells were treated with serum-free medium for 12 h followed by LPS (1 μg/ml) for 12 h in the LPS group; cells were treated with serum-free medium for 12 h followed by PB2 (5 μg/ml) for 12 h in the PB2 group; cells were treated with serum-free medium for 12 h followed by PDTC (2 μg/ml) for 12 h in the PDTC group; cells were treated with PB2 (5 μg/ml) for 12 h followed by LPS (1 μg/ml) for 12 h in the LPS + PB2 group; cells were treated with PDTC (2 μg/ml) for 12 h followed by LPS (1 μg/ml) for 12 h in the LPS + PDTC group. Protein expression levels in HUVECs were (A) determined via western blotting and semi-quantified for (B) p-IκB-α/total IκB-α, (C) p-IκB-β/total IκB-β and (D) p-NF-κB p65/total NF-κB p65. β-actin was used as the loading control. Data are presented as the mean ± SD of at least three independent experiments run in triplicate (n=3). Data were analysed using one-way ANOVA followed by Tukey's post hoc test. **P<0.01 vs. vehicle control; $^{\#}$P<0.05, $^{\#\#}$P<0.01 vs. LPS. LPS, lipopolysaccharide; PB2, procyanidin B2; PDTC, pyrrolidinedithiocarbamate ammonium; p, phosphorylated; HUVEC, human umbilical vein endothelial cell.

Activation of NF-κB involves the phosphorylation and nuclear translocation of NF-κB p65 protein (39). Therefore, the protein expression levels of p-IκB-α, total IκB-α, p-IκB-β, total IκB-β, p-NF-κB p65 and total NF-κB p65 in HUVECs were determined via western blotting (Fig. 7). LPS significantly upregulated the protein expression levels of p-NF-κB p65, p-IκB-α and p-IκB-β compared with the vehicle control group in HUVECs. Pretreatment of LPS-treated cells with PB2 clearly reversed LPS-mediated alterations to p-NF-κB p65, p-IκB-α and p-IκB-β protein expression levels in HUVECs. In addition, pretreatment of LPS-treated cells with PDTC, a potent inhibitor of NF-κB, also notably reversed LPS-mediated alterations to p-NF-κB p65, p-IκB-α and p-IκB-β protein expression levels in HUVECs. The results suggested that the antiapoptotic effect of PB2 might be mediated via regulation of NF-κB signalling pathway-related proteins in HUVECs.

Effect of PB2 on the phosphorylation and nuclear translocation of NF-κB p65 in HUVECs. Activation of NF-κB signalling is associated with the translocation of the NF-κB p65 protein from the cytoplasm into the nucleus, which is required for the release of cytokines and the expression of apoptosis-related proteins (15). Thus, the localization of NF-κB p65 in HUVECs was investigated (Fig. 8). Compared with the vehicle control, PB2 and PDTC groups, LPS induced significant translocation of NF-κB p65 from the cytoplasm to the nucleus in HUVECs. However, pretreatment of LPS-treated cells with PB2 or PDTC clearly inhibited LPS-induced nuclear translocation of NF-κB p65 in HUVECs. The results demonstrated that PB2 and PDTC effectively inhibited LPS-induced nuclear translocation of NF-κB p65 in HUVECs, indicating that the antiapoptotic effects of PB2 and PDTC might be mediated via suppressing the NF-κB signalling pathway in HUVECs.

Discussion

The active ingredients from natural plants display a variety of biological effects and thus have received increasing attention for the development of novel therapeutics for various diseases (40). Numerous studies have reported that medicines extracted from natural plants typically display fewer side effects compared with traditional medicines (41-44). Procyanidins are widely present in plants and are composed of a monomer, oligoprocyanidins and polymer proeyanidins (45). PB2 displayed potential pharmacological activity and a multitude of beneficial effects, including scavenging free radicals, antioxidation, anticancer, anti-inflammation, antiapoptosis and antiatherosclerosis effects (31). However, the molecular mechanism underlying the antiapoptotic effects mediated by PB2 is not completely understood.

The present study demonstrated that pretreatment with PB2 significantly attenuated LPS-mediated inhibition of cell

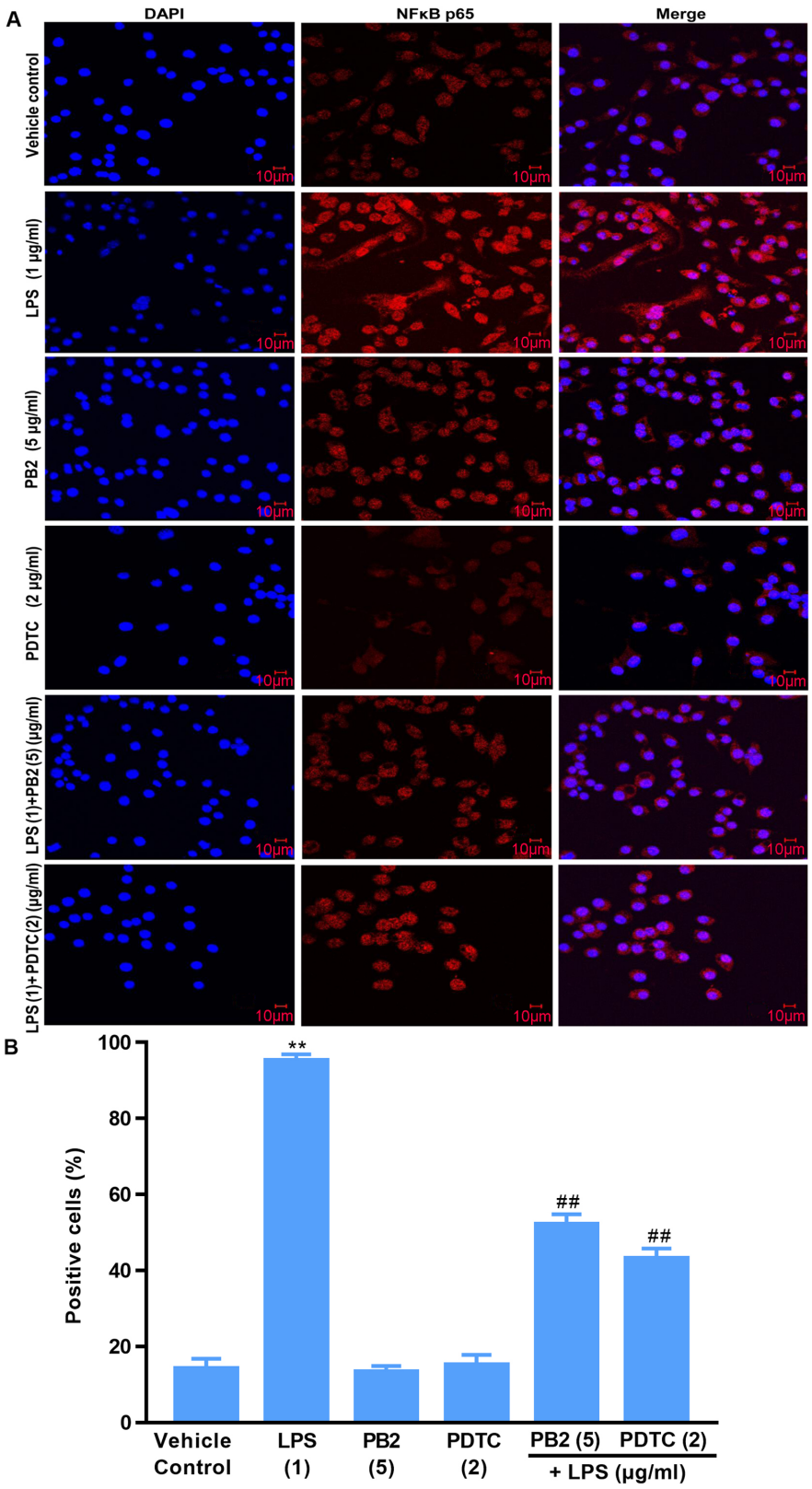

Figure 8. Effects of LPS, PB2 and PDTC on the nuclear translocation of NF-κB p65 in HUVECs. Cells were treated with serum-free medium for 24 h in the vehicle control group; cells were treated with serum-free medium for 12 h followed by LPS (1 μg/ml) for 12 h in the LPS group; cells were treated with serum-free medium for 12 h followed by PB2 (5 μg/ml) for 12 h in the PB2 group; cells were treated with serum-free medium for 12 h followed by PDTC (2 μg/ml) for 12 h in the PDTC group; cells were treated with PB2 (5 μg/ml) for 12 h followed by LPS (1 μg/ml) for 12 h in the LPS + PB2 group; cells were treated with PDTC (5 μg/ml) for 12 h followed by LPS (1 μg/ml) for 12 h in the LPS + PDTC group. (A) Representative images of the nuclear translocation of NF-κB p65 in HUVECs identified via immunofluorescence (magnification, x400). (B) Quantification of the percentage of positive cells with nuclear translocation of NF-κB p65. LPS markedly increased the translocation of NF-κB p65 from the cytoplasm to the nucleus compared with the control, PB2 and PDTC groups in HUVECs. However, pretreatment with PB2 or PDTC markedly inhibited LPS-induced translocation of NF-κB p65 in HUVECs. Data are presented as the mean ± SD of at least three independent experiments run in triplicate (n=3). Data were analysed using one-way ANOVA followed by Tukey's post hoc test. **P<0.01 vs. vehicle control; $^{\#\#}$P<0.01 vs. LPS. LPS, lipopolysaccharide; PB2, procyanidin B2; PDTC, pyrrolidinedithiocarbamate ammonium; HUVEC, human umbilical vein endothelial cell.

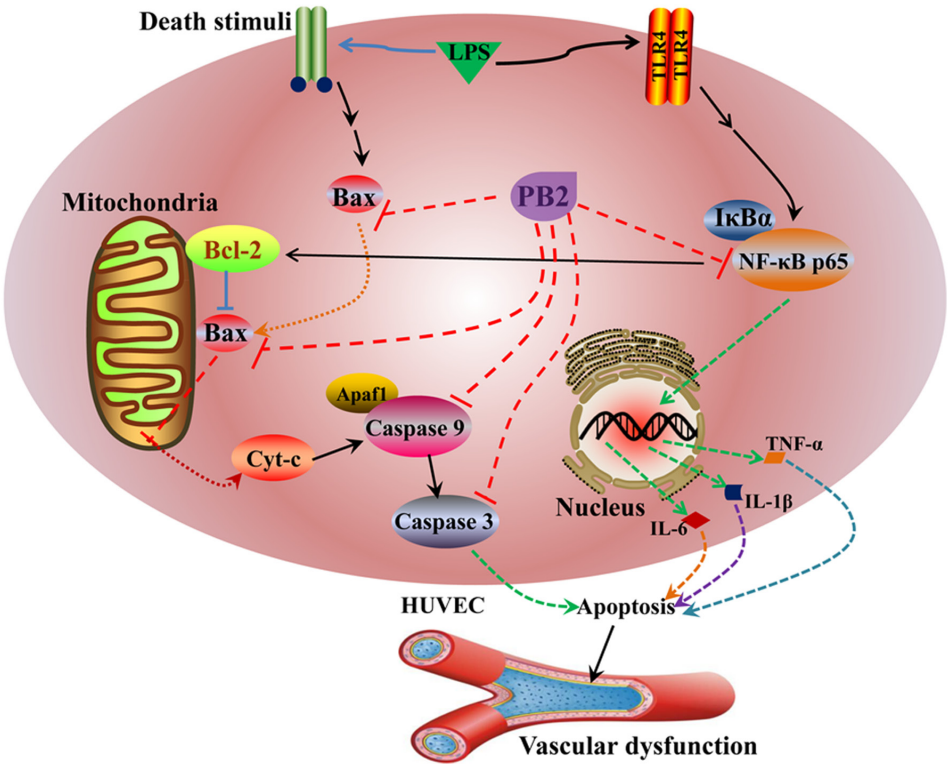

Figure 9. Proposed molecular mechanism underlying the effects of PB2 on LPS-induced inhibition of cell viability and apoptosis in HUVECs. PB2, procyanidin B2; LPS, lipopolysaccharide; Cyt-c, cytochrome *c*; Apaf1, apoptotic peptidase activating factor 1; HUVEC, human umbilical vein endothelial cell.

viability, although PB2 (≤5 μg/ml) did not display cytotoxic effects on HUVECs. The results indicated the protective effect of PB2 against LPS-induced cytotoxicity in HUVECs. Furthermore, PB2 markedly reduced the cell apoptotic ratio from >70% in the LPS group to <10% in the LPS + PB2 group. The Hoechst 33258 staining assay results indicated the protective effect of PB2 on LPS-mediated inhibition of cell viability might be mediated via its antiapoptotic effect in HUVECs. In addition, LPS significantly decreased the mitochondrial membrane potential compared with the vehicle control group, but PB2 reversed LPS-induced reductions in the mitochondrial membrane potential in HUVECs. The results suggested that the antiapoptotic effect of PB2 on LPS-induced HUVECs was associated with regulation of the mitochondrial membrane potential.

Key proinflammatory cytokines, such as IL-1β, IL-6 and TNF-α, serve an important role in the immune response to inflammation and are closely related to a variety of cellular activities including proliferation, differentiation and apoptosis (36,46,47). Therefore, the effects of PB2 on LPS-induced upregulation of IL-1β, IL-6 and TNF-α mRNA and protein expression levels were assessed by performing RT-qPCR and ELISAs, respectively. The results demonstrated that compared with the vehicle control group, IL-1β, IL-6 and TNF-α protein levels were significantly increased to ~3050, 2780 pg/ml and 21.57 ng/ml by LPS, respectively. The results of the present study were consistent with a previous study that reported that the production of IL-1β, IL-6, and TNF-α was significantly increased by LPS in human monocytes/macrophages (37). Interestingly, pretreatment with PB2 or PDTC significantly decreased LPS-induced increases in IL-1β, IL-6 and TNF-α mRNA and protein expression levels in HUVECs. Therefore, the results of the present study demonstrated that PB2 and PDTC effectively inhibited LPS-induced upregulation of IL-1β, IL-6 and TNF-α mRNA expression and protein levels.

Bcl-2 and Bax genes are the most important genes in the regulation of apoptosis, and the Bcl-2/Bax signalling pathway serves an important role in the process of cellular apoptosis (7,8). The results of the present study indicated that compared with the vehicle control group, LPS significantly upregulated Bax, caspase-3, caspase-7 and caspase-9 expression levels, but markedly downregulated Bcl-2 protein expression levels in HUVECs. Interestingly, pretreatment with PB2 notably downregulated LPS-mediated alterations to protein expression levels in HUVECs. The results suggested that the inhibitory effect of PB2 against LPS-induced apoptosis might be associated with regulation of the Bax/Bcl-2 signalling pathway in HUVECs.

NF-κB serves an important role in stress, inflammation and immune response via control of DNA transcription, cell survival, apoptosis and cytokine production (48). IKK is rapidly activated and is responsible for the phosphorylation of IκB upon stimulation by external signals or stress, targeting IκB to ubiquitin-mediated protein degradation (49). IκB-α and IκB-β are the major signal-responsive isoforms in the IκB family that are responsible for promoting and terminating NF-κB activation during persistent stimulation (18). Therefore, the effects of PB2 on LPS-mediated alterations to IκB-α, IκB-β, p-NF-κB p65 and total NF-κB p65 protein expression levels, as well as the localization of NF-κB p65 in HUVECs were investigated. The results suggested that PB2 may serve a

crucial role in inhibiting LPS-induced upregulation of IκB-α, IκB-β, p-NF-κB p65 expression levels, and nuclear translocation of p-NF-κB p65.

The potential mechanisms underlying the protective effects of PB2 against LPS-induced cytotoxicity and apoptosis in HUVECs identified in the present study are presented in Fig. 9. However, the molecular mechanisms underlying the effects of PB2 are likely complicated, thus other cellular signalling pathways require further investigation. The present study provided novel insights into the protective effect of PB2 against LPS in HUVECs, which might be important for the pharmacological basis and future clinical application of PB2 for the treatment of infectious vascular diseases. However, the *in vitro* results of the present study require verification using appropriate *in vivo* animal models and clinical trials.

In conclusion, the present study suggested that LPS induced cytotoxicity and apoptosis in HUVECs by decreasing the mitochondrial membrane potential and upregulating the mRNA expression and protein levels of key proinflammatory cytokines, including IL-1β, IL-6 and TNF-α. Moreover, compared with the vehicle control group, LPS also significantly upregulated Bax, cleaved caspase-3, cleaved caspase-7, cleaved caspase-9 and p-NF-κB-p65 expression levels, but downregulated Bcl-2, p-IκB-α and p-IκB-β protein expression levels, and promoted the translocation of NF-κB p65 from the cytoplasm to nucleus in HUVECs. Interestingly, PB2 attenuated LPS-induced cytotoxicity and apoptosis, and reversed LPS-mediated reductions in the mitochondrial membrane potential in HUVECs. PB2 also clearly inhibited LPS-induced upregulation of Bax, cleaved caspase-3, cleaved caspase-7, cleaved caspase-9, p-IκB-α, p-IκB-β and p-NF-κB-p65 expression levels, and reversed LPS-induced downregulation of Bcl-2 protein expression levels. Furthermore, PB2 inhibited LPS-induced NF-κB p65 translocation from the cytoplasm to the nucleus in HUVECs. The possible molecular mechanism underlying the protective effects of PB2 against LPS-induced cytotoxicity and apoptosis in HUVECs might be mediated via inhibiting the Bcl-2/Bax and NF-κB signalling pathways. Therefore, PB2 may serve as a novel therapeutic agent for infectious vascular diseases.

Acknowledgements

Not applicable.

Funding

This study was supported by the Education Department of Sichuan Province (grant nos. 13ZB0267 and 14ZA0143), the Joint Research Fund of Technology Bureau of Luzhou City Government and Luzhou Medical University (grant nos. 14JC0181 and 2013LZLY-J52) and the Distinguished Professor Research Startup Funding (S. Cao) from Southwest Medical University (grant no. 2015-RCYJ0002).

Availability of data and materials

The datasets used and/or analysed during the current study are available from the corresponding author on reasonable request.

Authors' contributions

XJ and SSC designed the experiments and analysed the data. DQS, FW, MHL, XFL, JL and ZZ performed the experiments. DQS and SSC wrote the manuscript. All authors discussed the results. DQS, JL, FW, SSC and XJ confirmed the authenticity of all the raw data. All authors read and approved the final manuscript.

Ethics approval and consent to participate

Not applicable.

Patient consent for publication

Not applicable.

Competing interests

The authors declare that they have no competing interests.

References

1. Gimbrone MJ and García-Cardeña G: Endothelial cell dysfunction and the pathobiology of atherosclerosis. Circ Res 118: 620-636, 2016.
2. Yao Z, Mates JM, Cheplowitz AM, Hammer LP, Maiseyeu A, Phillips GS, Wewers MD, Rajaram MV, Robinson JM, Anderson CL and Ganesan LP: Blood-borne lipopolysaccharide is rapidly eliminated by liver sinusoidal endothelial cells via high-density lipoprotein. J Immunol 197: 2390-2399, 2016.
3. Li L, Wan G, Han B and Zha ZW: Echinacoside alleviated LPS-induced cell apoptosis and inflammation in rat intestine epithelial cells by inhibiting the mTOR/STAT3 pathway. Biomed Pharmacother 104: 622-628, 2018.
4. Liang Z and Ren C: Emodin attenuates apoptosis and inflammation induced by LPS through up-regulating lncRNA TUG1 in murine chondrogenic ATDC5 cells. Biomed Pharmacother 103: 897-902, 2018.
5. Ma H, Su L, He X and Miao J: Loss of HMBOX1 promotes LPS-induced apoptosis and inhibits LPS-induced autophagy of vascular endothelial cells in mouse. Apoptosis 24: 946-957, 2019.
6. Mohan S, Abdelwahab SI, Kamalidehghan B, Syam S, May KS, Harmal NS, Shafifiyaz N, Hadi AH, Hashim NM, Rahmani M, *et al*: Involvement of NF-κB and Bcl2/Bax signaling pathways in the apoptosis of MCF7 cells induced by a xanthone compound Pyranocycloartobiloxanthone A. Phytomedicine 19: 1007-1015, 2012.
7. Lindsay J, Esposti MD and Gilmore AP: Bcl-2 proteins and mitochondria-specificity in membrane targeting for death. Biochim Biophys Acta 1813: 532-539, 2011.
8. Chalah A and Khosravi-Far R: The mitochondrial death pathway. Adv Exp Med Biol 61: 525-545, 2008.
9. Zhang Z, Liang Z, Li H, Li C, Yang Z, Li Y, She D, Cao L, Wang W, Liu C and Chen L: Perfluorocarbon reduces cell damage from blast injury by inhibiting signal paths of NF-κB, MAPK and Bcl-2/Bax signaling pathway in A549 cells. PLoS One 12: e0173884, 2017.
10. Zhang Y, Yang X, Ge XH and Zhang FY: Puerarin attenuates neurological deficits via Bcl-2/Bax/cleaved caspase-3 and Sirt3/SOD2 apoptotic pathways in subarachnoid hemorrhage mice. Biomed Pharmacother 109: 726-733, 2019.
11. Lin P, Zhou B, Yao HY and Guo YP: Effect of carboplatin injection on Bcl-2 protein expression and apoptosis induction in Raji cells. Eur J Histochem 64: 3134, 2020.
12. Mao ZX, Xia W, Wang J, Chen T, Zeng Q, Xu B, Li W, Chen X and Xu S: Perfluorooctane sulfonate induces apoptosis in lung cancer A549 cells through reactive oxygen species-mediated mitochondrion-dependent pathway. J Appl Toxicol 33: 1268-1276, 2013.
13. Ke WW, Zhao XX and Lu ZM: Foeniculum vulgare seed extract induces apoptosis in lung cancer cells partly through the down-regulation of Bcl-2. Biomed Pharmacother 135: 111213, 2021.

14. Parrish AB, Freel CD and Kornbluth S: Cellular mechanisms controlling caspase activation and function. Cold Spring Harb Perspect Biol 5: a008672, 2013.
15. Hoesel B and Schmid JA: The complexity of NF-κB signaling in inflammation and cancer. Mol Cancer 12: 86, 2013.
16. Zhu DD, Zhang J, Deng W, Yip YL, Lung HL, Tang CM, Law WT, Yang J, Lau VM, Shuen WH, *et al*: Significance of NF-κB activation in immortalization of nasopharyngeal epithelial cells. Int J Cancer 138: 1175-1185, 2016.
17. Liu Y, Zhou G, Wang Z, Guo X, Xu Q, Huang Q and Su L: NF-κB signaling is essential for resistance to heat stress-induced early stage apoptosis in human umbilical vein endothelial cells. Sci Rep 5: 135147, 2015.
18. Hoffmann A and Baltimore D: Circuitry of nuclear factor KappaB signaling. Immunol Rev 210: 171-186, 2006.
19. Sun SC, Ganchi PA, Ballard DW and Greene WC: NF-kappa B controls expression of inhibitor I kappa B alpha: Evidence for an inducible autoregulatory pathway. Science 259: 1912-1915, 1993.
20. Arenzana-Seisdedos F, Thompson J, Rodriguez MS, Bachelerie F, Thomas D and Hay RT: Inducible nuclear expression of newly synthesized I kappa B alpha negatively regulates DNA-binding and transcriptional activities of NF-kappa B. Mol Cell Biol 15: 2689-2696, 1995.
21. Perkins ND: Integrating cell-signalling pathways with NF-kappaB and IKK function. Rev Mol Cell Biol 8: 49-62, 2007.
22. Sakano K, Mizutani M, Murata M, Oikawa S, Hiraku Y and Kawanishi S: Procyanidin B2 has anti-and pro-oxidant effects on metal-mediated DNA damage. Free Radic Biol Med 39: 1041-1049, 2005.
23. Gopalakrishnan S, Ediga HH, Reddy SS, Reddy GB and Ismail A: Procyanidin-B2 enriched fraction of cinnamon acts as a proteasome inhibitor and anti-proliferative agent in human prostate cancer cells. IUBMB Life 70: 445-457, 2018.
24. Chai WM, Lin MZ, Feng HL, Zou ZR and Wang YX: Proanthocyanidins purified from fruit pericarp of *Clausena lansium* (Lour.) Skeels as efficient tyrosinase inhibitors: Structure evaluation, inhibitory activity and molecular mechanism. Food Funct 8: 1043-1051, 2017.
25. Liu D: Effects of procyanidin on cardiomyocyte apoptosis after myocardial ischemia reperfusion in rats. BMC Cardiovasc Disord 18: 351, 2018.
26. Yang H, Xiao L, Yuan Y, Luo X, Jiang M, Ni J and Ni JH: Procyanidin B2 inhibits NLRP3 inflammasome activation in human vascular endothelial cells. Biochem Pharmacol 92: 599-606, 2014.
27. Jiang Y, Wang X, Yang W and Gui S: Procyanidin B2 suppresses Lipopolysaccharides-induced inflammation and apoptosis in human type II alveolar epithelial cells and lung fibroblasts. J Interferon Cytokine Res 40: 54-63, 2020.
28. Li XL, Li BY, Cheng M, Yu F, Yin WB, Cai Q, Zhang Z, Zhang JH, Wang JF, Zhou RH and Gao HQ: PIMT prevents the apoptosis of endothelial cells in response to glycated low density lipoproteins and protective effects of grape seed procyanidin B2. PLoS One 8: e69979, 2013.
29. Wu QJ, Wang YQ and Qi YX: The protective effect of procyanidin against LPS-induced acute gut injury by the regulations of oxidative state. Springerplus 5: 1645, 2016.
30. Dong F, Zhou X, Li C, Yan S, Deng X, Cao Z, Li L, Tang B, Allen TD and Liu J: Dihydroartemisinin targets VEGFR2 via the NF-κB pathway in endothelial cells to inhibit angiogenesis. Cancer Biol Ther 15: 1479-1488, 2014.
31. Zhang JQ, Gao WB, Wang J, Ren QL, Chen JF, Ma Q, Zhang ZJ and Xing BS: Critical role of FoxO1 in granulosa cell apoptosis caused by oxidative stress and protective effects of grape seed procyanidin B2. Oxid Med Cell Longev 2016: 6147345, 2016.
32. Martinez-Micaelo N, González-Abuín, N, Pinent M, Ardévol N and Blay M: Procyanidin B2 inhibits inflammasome-mediated IL-1β production in lipopolysaccharide-stimulated macrophages. Mol Nutr Food Res 59: 262-269, 2015.
33. Livak KJ and Schmittgen TD: Analysis of relative gene expression data using real-time quantitative PCR and the 2(-Delta Delta C(T)) method. Methods 25: 402-408, 2001.
34. Crews L and Masliah E: Molecular mechanisms of neurodegeneration in Alzheimer's disease. Hum Mol Genet 19: R12-R20, 2010.
35. Wlodkowic D, Telford W, Skommer J and Darzynkiewicz Z: Apoptosis and beyond: Cytometry in studies of programmed cell death. Methods Cell Biol 103: 55-98, 2011.
36. Troy CM and Jean YY: Caspases: Therapeutic targets in neurologic disease. Neurotherapeutics 12: 42-48, 2015.
37. Zou H, Li Y, Liu X and Wang X: An APAF-1 cytochrome *c* multimeric complex is a functional apoptosome that activates procaspase-9. J Biol Chem 274: 11549-11556, 1999.
38. Robertson JD, Orrenius S and Zhivotovsky B: Review: Nuclear events in apoptosis. J Struct Biol 129: 346-358, 2000.
39. Christian F, Smith EL and Carmody RJ: The regulation of NF-κB subunits by phosphorylation. Cells 5: 12, 2016.
40. Sellami M, Slimeni O, Pokrywka A, Kuvačić G, D Hayes L, Milic M and Padulo J: Herbal medicine for sports: A review. J Int Soc Sports Nut 15: 14, 2018.
41. Shen CY, Jiang JG, Yang L, Wang DW and Zhu W: Anti-ageing active ingredients from herbs and nutraceuticals used in traditional Chinese medicine: Pharmacological mechanisms and implications for drug discovery. Br J Pharmacol 174: 1395-1425, 2017.
42. Wang YS, Shen CY and Jiang JG: Antidepressant active ingredients from herbs and nutraceuticals used in TCM: Pharmacological mechanisms and prospects for drug discovery. Pharmacol Res 150: 104120, 2019.
43. Hughes K, Ho R, Butaud JF, Filaire E, Ranouille E, Berthon JY and Raharivelomanana P: A selection of eleven plants used as traditional Polynesian cosmetics and their development potential as anti-aging ingredients, hair growth promoters and whitening products. J Ethnopharmacol 245: 112159, 2019.
44. Gordobil O, Olaizola P, Banales JM and Labidi J: Lignins from Agroindustrial by-products as natural ingredients for cosmetics: Chemical structure and in vitro sunscreen and cytotoxic activities. Molecules 25: 1131, 2020.
45. Hollands WJ, Voorspoels S, Jacobs G, Aaby K, Meisland A, Garcia-Villalba R, Tomas-Barberan F, Piskula MK, Mawson D, Vovk I, *et al*: Development, validation and evaluation of an analytical method for the determination of monomeric and oligomeric procyanidins in apple extracts. J Chromatogr A 1495: 46-56, 2017.
46. Wan FY and Lenardo MJ: The nuclear signaling of NF-kappaB: Current knowledge, new insights, and future perspectives. Cell Res 20: 24-33, 2010.
47. Tanaka T, Narazaki M and Kishimoto T: IL-6 in inflammation, immunity, and disease. Cold Spring Harb Perspect Biol 6: a016295, 2014.
48. Yang HJ, Wang M, Wang L, Cheng BF, Lin XY and Feng ZW: NF-κB regulates caspase-4 expression and sensitizes neuroblastoma cells to Fas-induced apoptosis. PLoS One 10: e0117953, 2015.
49. Verhoeven RJ, Tong S, Zhang G, Zong J, Chen Y, Jin DY, Chen MR, Pan J and Chen H: NF-κB signaling regulates expression of Epstein-Barr virus BART microRNAs and long noncoding RNAs in nasopharyngeal carcinoma. J Virol 90: 6475-6488, 2016.